Journal of Applied Polymer Science

Study on the Preparation and Thermal Shrinkage Properties of Nano-SiO_2/UHMWPE/HDPE Blend Microporous Membranes

Yin-Cai Wu,[1] Yi-Hua Cui,[1] Huai-Long Jin,[2] Chong-Chong Ning[1]

[1]College of Materials Science and Technology, Nanjing University of Aeronautics and Astronautics, Nanjing 210016, China

[2]NanJing LanPuCheng Industrial Co., Ltd. 211100, China

Correspondence to: Y.-C. Wu (E-mail: cuiyh@nuaa.edu.cn)

ABSTRACT: Nano-SiO_2/UHMWPE/HDPE blend microporous membranes (NBMs) with different content of nano-SiO_2 particles were prepared via thermally induced phase separation process. Thermogravimetric analysis was used to investigation of the amount of nano-SiO_2 particles reserved in NBMs. This approach showed that about 59% of total content of nano-SiO_2 particles reserved in NBMs. The formation and development of the interface pores were studied by scanning electron microscopy. NBMs performance was characterized by a variety of metrics including thermal shrinkage, melting and crystallization behavior, porosity and pore diameter, and permeability. The results indicated that nano-SiO_2 particles served as nucleating agent increasing the crystalline of NBMs. The comprehensive properties of NBMs were optimum when the content of nano-SiO_2 particles was 1%. Compared with pure HDPE separators, NBMs exhibit higher porosity and lower thermal shrinkage due to its high crystalline and the enrichment of UHMWPE chains. © 2014 Wiley Periodicals, Inc. J. Appl. Polym. Sci. **2015**, *132*, 41321.

KEYWORDS: blends; films; membranes; porous materials; surfaces and interfaces

Received 19 February 2014; accepted 22 July 2014

DOI: 10.1002/app.41321

INTRODUCTION

From the viewpoint of lithium-ion battery safety, the separator is considered to be a key component to suppress undesirable collapses, as its primary function is to maintain physical isolation between the cathode and the anode.[1,2] High density polyethylene (HDPE)-based separators are widely and offer many advantages such as good mechanical properties, corrosion resistance, and low price.[3] HDPE separator guarantees the lower shutdown temperature because of its low melting point. Nevertheless, its poor thermal stability has raised serious concerns over its ability to maintain the necessary electrical isolation between electrodes, particularly under harsh conditions such as abnormal heating or mechanical rupture.

To overcome these drawbacks above, it is necessary to modify the thermal shrinkage of HDPE separator. Lots of approaches have been carried out such as surface coating modification[4,5] and chemically surface grafting modification.[6,7] Although the thermal shrinkage of HDPE separator can be improved via these operations, the coating or grafting modification layer might lead to the thickness increasing and pore blocking, which would deteriorate the performance of separators on the contrary.[3] Blending method is another convenient way to modify the thermal shrinkage of separators, which can avoid the thickness increasing and pore blocking as mentioned above. It can not only keep shutdown temperature low but also reduce the thermal shrinkage of separators by selecting the optimum blending reagent and preparation conditions.

The thermally induced phase separation (TIPS) process has been studied extensively on fabricating the microporous membranes of semicrystalline polymers such as polyethylene (PE),[6,8–10] polypropylene,[11,12] and polyvinylidene fluoride.[13,14] In the TIPS process, the homogeneous polymer-diluent mixture is prepared by melting mixture at a relatively high temperature, then liquid–liquid or solid–liquid phase is separated with the decreasing of temperature. The microporous membranes are formed by removing diluent droplets from membranes. When the size of droplet diluent was controlled, pore size of microporous membranes can be adjusted.[15] The advantage of TIPS is that it can incorporate the second phase components into the mixed solution, so that the chemical or physical reaction can occur between second phase and matrix. Thus, the performance of matrix membranes may be modified.

Ultra high molecular weight polyethylene (UHMWPE) has the excellent chemical corrosion resistance, high temperature mechanical properties, and low thermal shrinkage. The morphology and mechanical properties of HDPE can be changed by blending with a certain amount of UHMWPE.[16] Nano-SiO_2 particles have been widely used in the film industry, because its

Table I. The Composition of the NLPMS

Membranes	HDPE (wt %)	UHMWPE (wt %)	Nano-SiO_2 (wt %)	LP (wt %)	Antioxygen (wt %)
S-1	28.5	1.5	0	70	0.15
S-2	28.5	1.5	0.5	70	0.15
S-3	28.5	1.5	1	70	0.15
S-4	28.5	1.5	1.5	70	0.15
S-5	28.5	1.5	2	70	0.15

superiority in preventing thermal shrinkage and mechanical breakdown of the separators. In addition, the membranes with nano-SiO_2 were not easy bonded between each other, which facilitates winding in the actual production. In this article, nano-SiO_2/UHMWPE/HDPE blend microporous membranes (NBMs) were prepared by TIPS method. The research focused on the performance of thermal shrinkage and microporous structure of NBMs with the variable amount of nano-SiO_2 particles.

EXPERIMENTAL

Materials

HDPE (B5429) was purchased from SABIC Innovative Plastics Co., Ltd. (China). UHMWPE (M_w=320 W) was purchased from Mitsui Chemicals Co., Ltd. (China). LP was provided by Qingdao Huashan Oil Co., Ltd. (China). Nano-SiO_2 with average size of 20 nm was purchased from Nanjing Crown Industry Co., Ltd. (China). Hexane and alcohol were provided by Nanjing Chemical Reagent Co., Ltd. (China).

Preparation of NBMs

First, the nano-SiO_2/UHMWPE/HDPE/LP mixture samples (NLPMS) were prepared as follows: liquid paraffin, nano-SiO_2 particles, and antioxidant (the weight ratio as shown in Table I) were mixed at room temperature for 30 min using a KQ-400B ultrasonic device. Then, HDPE and UHMWPE were dissolved in the mixture of liquid paraffin/nano-SiO_2, kept stirring for 40 min at 180°C. After mixing process, the solution with the beaker was quenched in a water bath (25°C) for 30 min.

A total of 15 mg of solid NLPMS were placed between a pair of stainless steel plates. A piece of polyester film with a square opening (150 × 150 mm^2) in the center was inserted between two pieces of polyester film to adjust the average thickness of membrane to 80 μm, as shown in Figure 1. The NLPMS were heated up to 180°C for 5 min on the plate vulcanizing machine and pressed with 10 MPa of pressure. Then, the stainless steel plate with the film together was taken out quickly and quenched in a water bath (25°C) for 10 min.

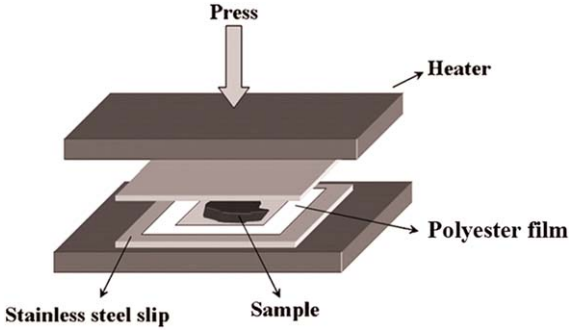

Figure 1. Schematic diagram of plate vulcanizing machine preparation of membranes. [Color figure can be viewed in the online issue, which is available at wileyonlinelibrary.com.]

The diluent in membranes was extracted by immersing membranes in *n*-hexane for 12 h. After taking out the membranes from the *n*-hexane, they were quickly fixed on a self-made wooden frame with a clamp. The final membranes were dried under vacuum at 50°C for 12 h, and then the membranes were placed in vacuum drying chamber at 100°C for 3 min to release the thermal stress.

Table I lists the weight ratio of HDPE, UHMWPE, nano-SiO_2 particles, and LP in all NLPMS. All of NLPMS contained 30 wt % polymers and (0 wt %, 0.5 wt %, 1 wt %, 1.5 wt %, 2 wt %) nano-SiO_2 particles of total concentration with various HDPE/UHMWPE: nano-SiO_2 ratios. For simplicity, the final NBMs with containing 0 wt %, 0.5 wt %, 1 wt %, 1.5 wt %, and 2 wt % nano-SiO_2 particles were named as S-1, S-2, S-3, S-4, and S-5, respectively.

Morphologies of NBMs

The morphologies of the surface and the cross-section of the NBMs were observed by a JSM-6360LV Scanning Electron Microscopy, respectively. NBMs were fractured in liquid

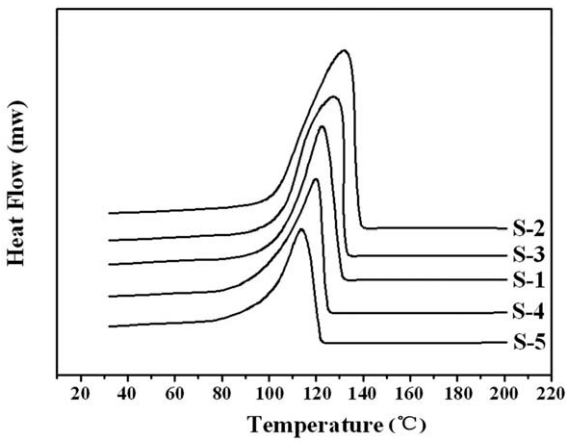

Figure 2. Effects of the amount of the nano-SiO_2 particles on the DSC curves of NLPMS.

Table II. The Thermal Analysis Data of the NLPMS

Samples	Fusion temperature (°C)	Melting enthalpy (J/g)	Crystallinity (%)
S-1	121.57	137.81	48.00
S-2	127.28	146.42	51.26
S-3	133.21	157.91	55.56
S-4	118.11	132.06	46.70
S-5	113.43	117.71	41.84

nitrogen and coated with a thin layer of gold by sputtering before observation.

Differential Scanning Calorimetry Experiment

The melting point and crystalline of the NLPMS were characterized by a STA409 PC differential scanning calorimetry (DSC). The NLPMS were heated from 30 to 200°C at a heating rate of 10°C/min under nitrogen atmosphere. The crystalline was calculated according to crystal melting enthalpy of membrane by eq. (1)[17]

$$X_c(\%) = \frac{\Delta H_f}{\Delta H_f^* \times \varphi} \quad (1)$$

where X_c is the crystalline of membrane, ΔH_f^* is the melting enthalpy of pure crystal, ΔH_f is the melting enthalpy of reality crystal, and φ is the ratio of polymer in NLPMS.

Thermo-Gravimetric Analysis Experiment

Thermo-gravimetric analysis (TGA) was characterized by a STA409 PC DSC. The NLPMS were heated from 30 to 850°C at a heating rate of 30°C/min under nitrogen atmosphere. Then, NLPMS temperature, weight and first derivative temperature were recorded.

Thermal Shrinkage

The thermal shrinkage of membrane was measured by putting NBMs in vacuum oven at 130°C for 1 h and then calculated by eq. (2)[18]

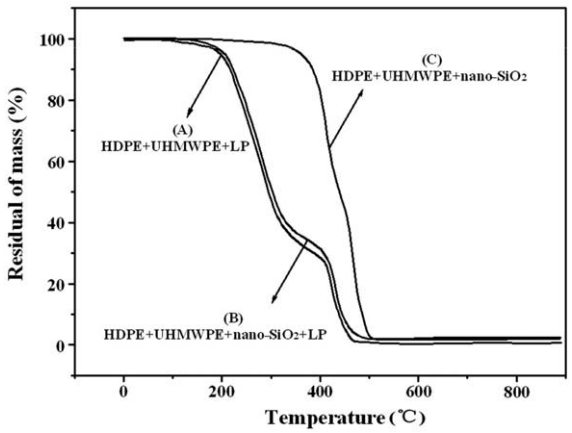

Figure 3. TGA curves of A, B, C samples.

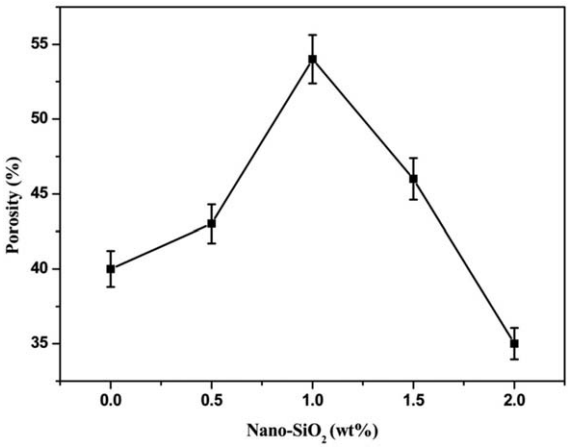

Figure 4. The relationship between the porosity of NBMs and the amount of nano-SiO_2 particles.

$$R(\%) = \frac{L}{L_o} \quad (2)$$

where R is thermal shrinkage rate of membrane, L is the after heating size of membrane, and L_o is the original size of membrane.

Porosity

The porosity of NBMs was measured according to the dry-wet weight ratio. The membranes were maintained in ethanol for 24 h then taken out and wiped superficial ethanol with filter paper before measuring the wet mass. Then, the wet membrane was placed in a vacuum oven at 80°C for 24 h before measuring the dry mass. According to the wet sample mass and the dry sample mass, the porosity of NBMs may be calculated by eq. (3)[10]

$$A_k(\%) = \frac{(W_2 - W_1)}{\rho W_2 + (\rho_1 - \rho_2) W_1} \quad (3)$$

where A_k is the porosity of NBMs, W_2 is the wet sample mass, W_1 is the dry sample mass, ρ_2 is the density of ethanol, and ρ_1 is the average density of NBMs. To minimize experimental error, each membrane was measured for three times, and then the average value was obtained.

Pure Water Flux

A cross flow filtration experimental apparatus was used to measure the PWF of NBMs. The apparatus was fed with distilled water at a trans-membrane pressure of 0.1 MPa after the membranes were prepressurized for 30 min at 0.15 MPa. The PWF may be calculated by eq. (4)[19,20]

$$F = \frac{V}{At} \quad (4)$$

where F is the pure water flux, V is the permeate volume, A is the membrane area, and t is the time.

RESULTS AND DISCUSSION

Thermal and Crystalline Properties of NLPMS

Figure 2 shows the DSC curves and Table II shows the thermal analysis data of NLPMS with different nano-SiO_2 particles contents. As shown in Figure 2 and Table II, the melting temperature and melting enthalpy of NLPMS increased at first and then

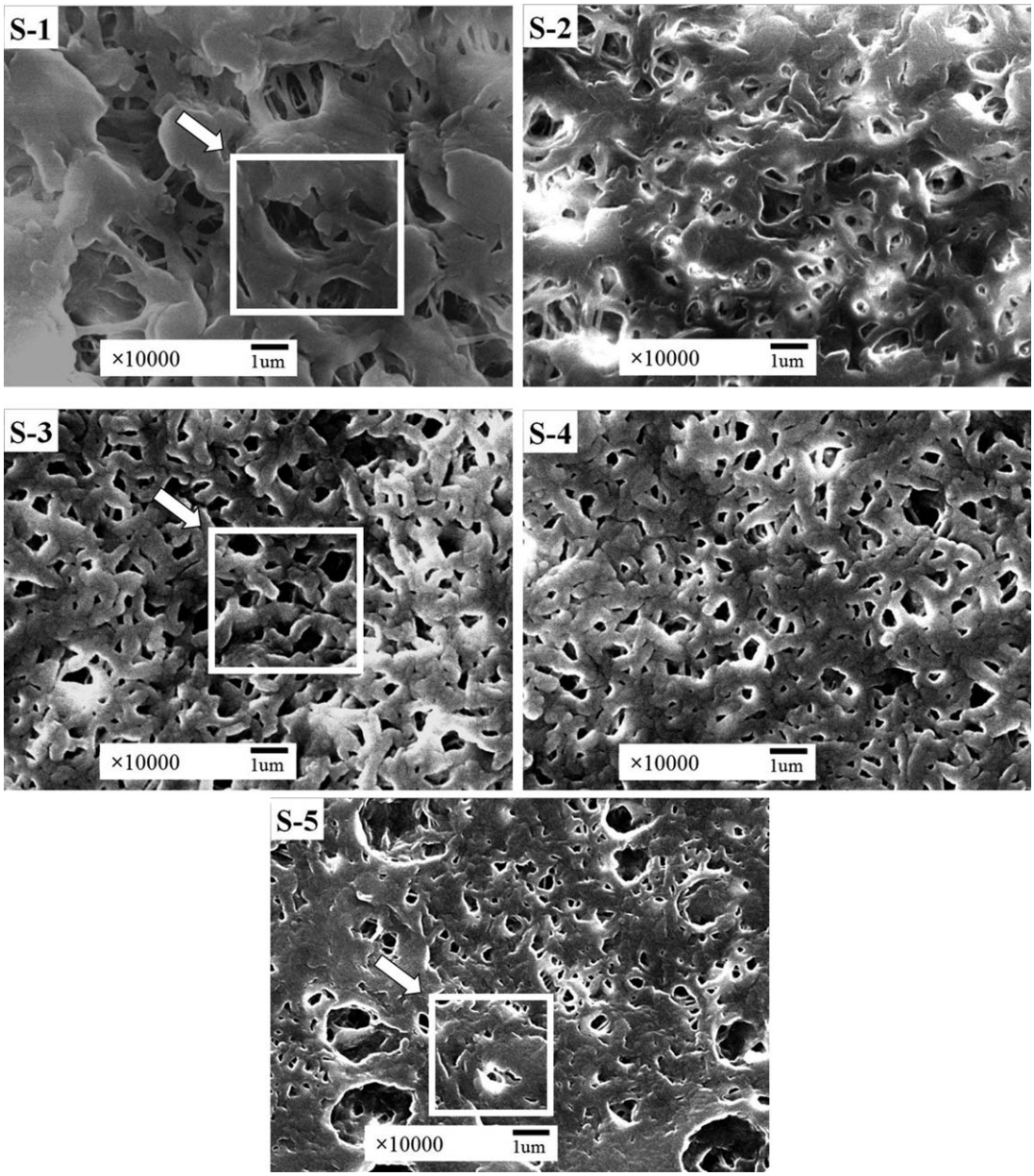

Figure 5. Surface morphology of the NBMs with different content of nano-SiO_2 particles.

decreased with nano-SiO_2 particles contents rising. This indicated that nano-SiO_2 particles influenced the thermodynamic stability of the NLPMS. Nano-SiO_2 particles could serve as heterogeneous nucleation in the NLPMS. The thermodynamic stability of heterogeneous nucleation was higher than that of homogeneous thermodynamic. Therefore, NLPMS with nano-SiO_2 particles were easily to crystallize at higher temperature. The improvement of molecular chains motion capacity and the crystallization rate of NLPMS benefit for high temperature of crystallization. Thus, the NLPMS were easily to form completed crystals so as to improve the crystalline of the NLPMS.[13]

The crystalline based on the heats of fusion was calculated according to eq. (1). The crystalline increased since ΔH_f^* was a constant and ΔH_f was increased when the amount of nano-SiO_2 particles was less than 1%. However, when the amount of nano-SiO_2 particles was more than 1%, the heterogeneous nucleation ability of nano-SiO_2 particles reduced and the homogeneous nucleation of the NLPMS were hindered instead, because nano-SiO_2 particles were easy to form agglomeration.

Thermal Decomposition Analysis

Figure 3 shows the TGA curves of blend samples. As shown in Figure 3, it can be obtain that the initial decomposed temperature of LP was about 210°C. From the curve (A), it can be concluded that the initial decomposed temperature of HDPE and UHMWPE was about 380°C for the NLPMS without nano-SiO_2 particles. By contrast, the initial decomposed temperature of HDPE and UHMWPE was about 405°C, which was 25°C higher than that of the NLPMS without nano-SiO_2 particles, for the

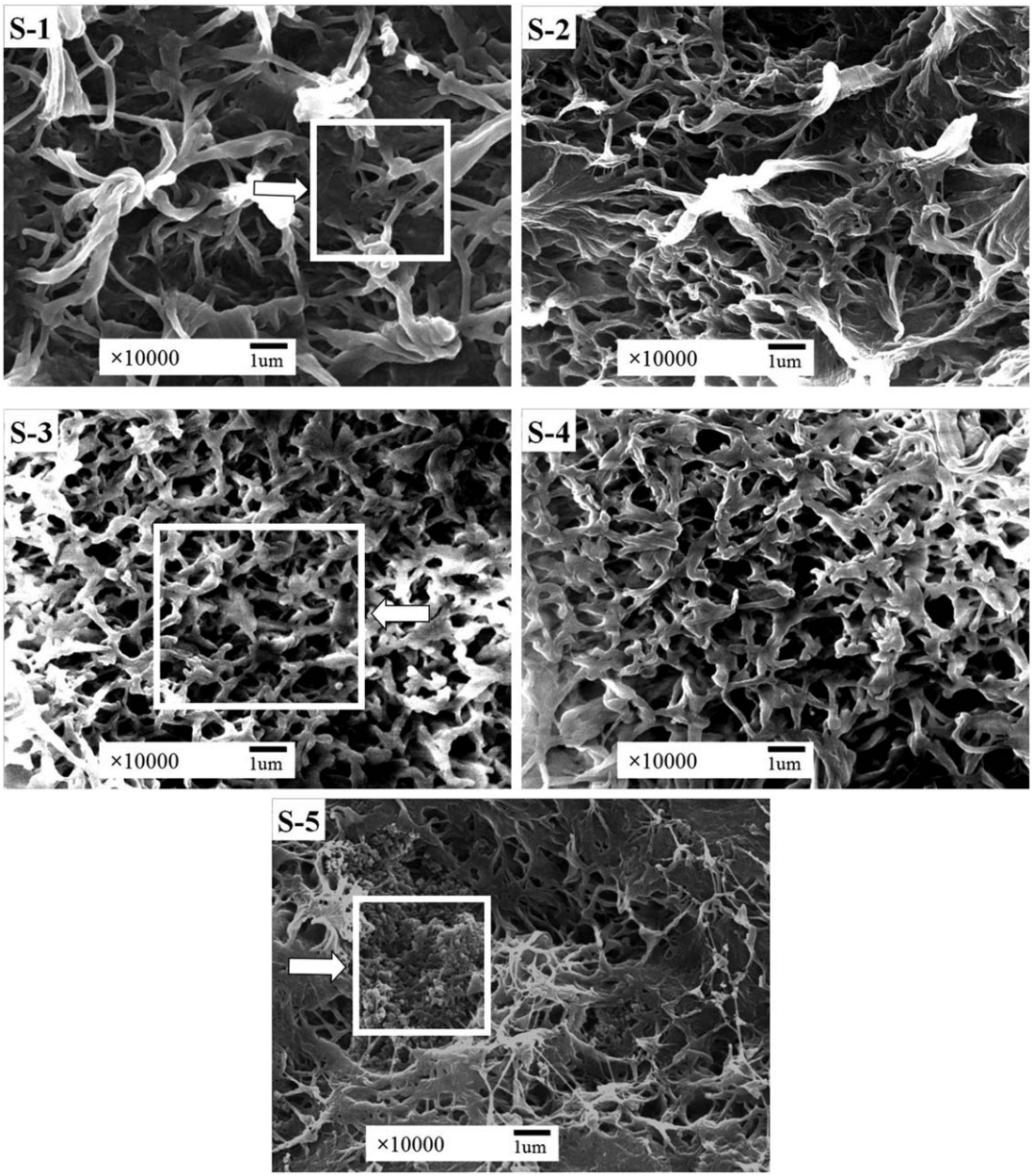

Figure 6. Cross-section morphology of the NBMs with different content of nano-SiO_2 particles.

NLPMS with 1% nano-SiO_2 particles as the curve (C) showed. From the above discussion, it was evident that nano-SiO_2 particles could enhance the thermal stability of NLPMS.[21] HDPE and UHMWPE had decomposed completely when the temperature reached 550°C. The residual mass of the NLPMS without nano-SiO_2 particles and with 1% nano-SiO_2 particles and the NBMs remain constant at 0, 0.894, and 0.527, respectively. Therefore, it was evident that during the preparation of NBMs, 41% of nano-SiO_2 particles acted as transitional role. Nano-SiO_2 particles firstly acted as nucleating agent to promote the crystallization of polymers matrix and then extracted with LP.

Porosity of NBMs

Figure 4 shows the effects of the amount of nano-SiO_2 particles on the porosity of the NBMs. As shown in Figure 4, the porosity of NBMs increased at first and then decreased. When the amount of nano-SiO_2 particles was 1%, the porosity might obtain the maximum value of 54%. When the amount of nano-SiO_2 particles was 1%.

The microporous framework of NBMs without nano-SiO_2 particles was easy to be shrinked. LP extraction from the NBMs caused the microporous to collapse easily, resulting in lower porosity. For NBMs with small amount of nano-SiO_2 particles, the strength of microporous framework were enhanced because the crystalline of NBMs increased as shown in Table II, resulting in large porosity and uniformity pore size. However, when the amount of nano-SiO_2 particles exceeded 1%, nano-SiO_2 particles began to aggregate, resulting in nonuniformity of crystallization. Nonuniformity of crystallization made the strength of

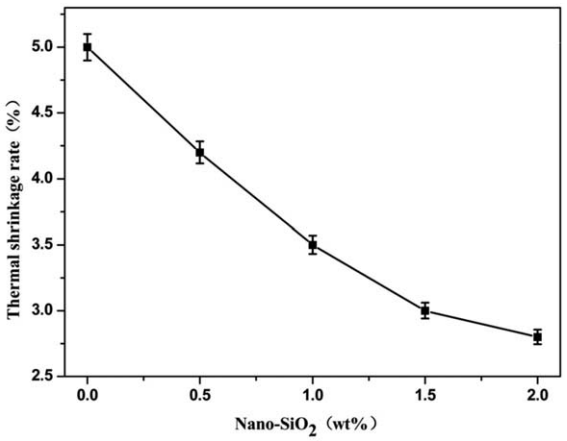

Figure 7. The relationship between thermal shrinkage of NBMs and the amount of nano-SiO_2 particles.

microporous framework of NBMs nonuniform, so microporous collapsing seriously and the pore size distributing nonuniformly.

Morphology Studies

Figure 5 shows the surface images and Figure 6 shows the cross-section images of the NBMs with different content of nano-SiO_2 particles. As shown in Figure 5 and Figure 6, the microporous structure of NBMs was significantly influenced by the content of nano-SiO_2 particles. When the content of nano-SiO_2 particles was less than 1%, the microporous of NBMs gradually increased in number and distributed more uniform with the increasing content of nano-SiO_2 particles. However, when the content of nano-SiO_2 particles exceeded 1%, the pore size of NBMs distributed nonuniform, rate of closed hole of the surface microporous and the cross-section microporous increased gradually.

The TIPS process of polymer solution included liquid–liquid phase separation, liquid–solid phase separation, and polymer crystallization.[22] The effect of inorganic nanoparticles on the microstructure of NBMs was mainly depended on the following two aspects. On the one hand, inorganic nanoparticles affected the phase separation of the blend solution system. A small amount of inorganic nanoparticles in the blend solution system played the role of the heterogeneous nucleation crystallization that reduced the crystallization enthalpy and made liquid–liquid phase separation temperature increase. At high temperature, the liquidity of the blend solution system was better, so the polymer-rich phase and the solvent-rich phase separated more easily. The increase of liquid–liquid phase separation temperature lengthens the solidification time, so the crystalline part of NLPMS more complete. Complete crystalline made the strength of microporous framework of NBMs enhance, resulting in more uniform structure and higher porosity. On the other hand, inorganic nanoparticles influenced the way of crystal formation, crystal process, and crystallization rate of the blend solution.[23] Thermodynamic and kinetic factors of the solution system determined the pore structure formation of the NBMs. Inorganic nanoparticles could improve the thermodynamic instability of the blend solution system and made the temperature of dynamic crystallization increase. A small amount of inorganic nanoparticles played the role of heterogeneous nucleation crystallization which reduced the interfacial free energy of crystallize nuclear, so the temperature of dynamic crystallization rose. When the content of inorganic nanoparticles exceeded a certain amount, the inorganic nanoparticles agglomerated seriously, the

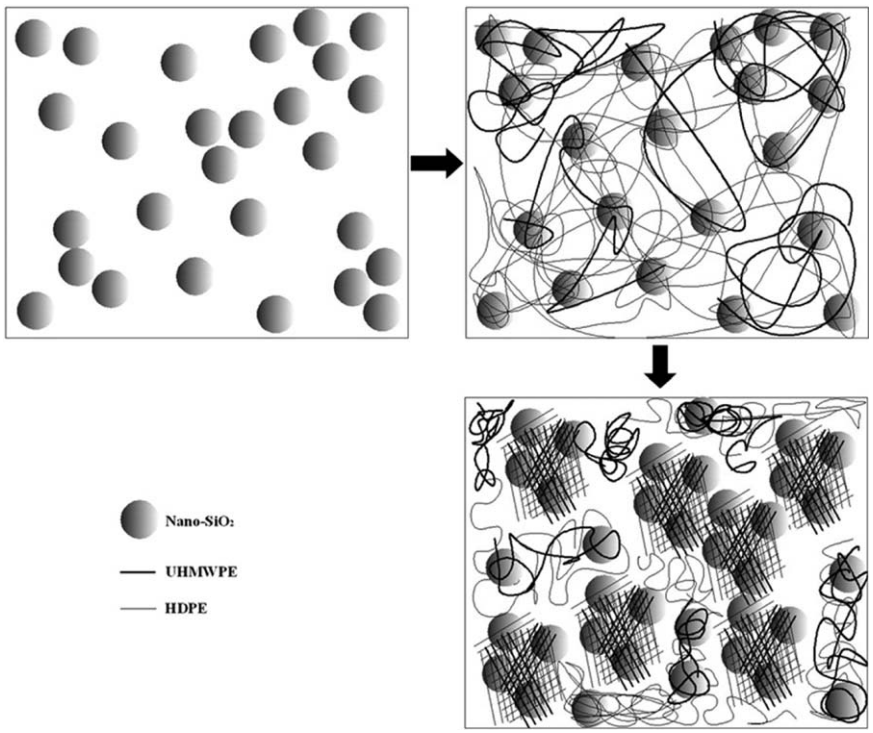

Figure 8. The schematic diagram of interaction between HDPE and UHMWPE molecular chains and nano-SiO_2 particles.

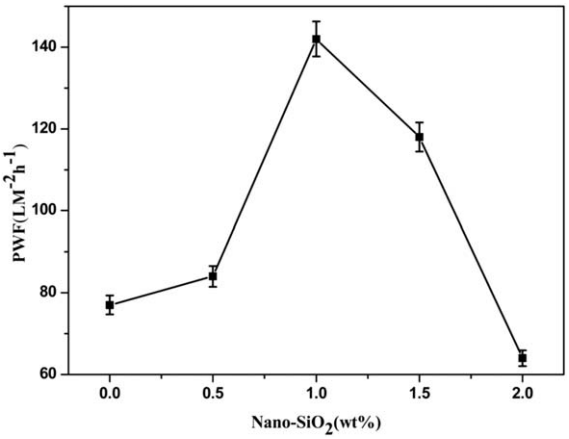

Figure 9. The relationship between PWF of NBMs and the amount of nano-SiO_2 particles.

temperature of dynamic crystallization declined and heterogeneous nucleation crystallization of the blend solution system became worse.[13]

Phase separation occurred in water-cooling condition followed by crystal process and grain growth process.[15] From the discussion above, it was evident that nano-SiO_2 particles in the blend solution system could play the role of heterogeneous nucleation crystallization. Liquid–liquid phase separation temperature and thermodynamic instability of the blend solution system improved for the affect of nano-SiO_2 particles. When the content of nano-SiO_2 particles were less than 1%, nano-SiO_2 particles act as nucleating agent to accelerate the rate of crystallization of the blend solution system, resulting in high porosity and uniform pore distribution of NBMs. However, when the nano-SiO_2 particles content exceeded 1%, nano-SiO_2 particles agglomerated seriously, the temperature of dynamic crystallization declined and heterogeneous nucleation crystallization of the blend solution system became worse. The crystallization rate of the blend solution system was very different, thus previous crystal grain swallowed the part of following crystal grain. The large crystallization region squeezed amorphous regions that caused the microporous of NBMs to close seriously, resulting in low porosity.[13,14]

Thermal Shrinkage Property

Nano-SiO_2 particles could improve the thermal stability of PE.[21] Figure 7 shows the relationship between thermal shrinkage of NBMs and the amount of nano-SiO_2 particles. As shown in Figure 7, the thermal shrinkage of the NBMs decreased with the increasing content of nano-SiO_2 particles.

UHMWPE and HDPE were semicrystalline polymers. During the formation process of NBMs, the crystalline behavior of blend solution system directly influenced the microporous skeleton strength of NBMs. Nano-SiO_2 particles played the role of nucleating agent that improved the crystallinity of the blend solution and enhanced the strength of microporous skeleton. In addition, UHMWPE and HDPE molecular chain intertwined with each other to form a network structure which packaged part of nano-SiO_2 particles on the network structure of the skeleton. The interaction between nano-SiO_2 particles and polymer chain by molecular force that limited the free movement of the UHMWPE and HDPE molecular chain (the interaction between HDPE molecular chain, UHMWPE molecular chain and nano-SiO_2 particles were shown in Figure 8). As a part of NBMs, nano-SiO_2 particles played the role of impeding thermal shrinkage of the HDPE and UHMWPE molecular chain when the molecular chains were heated. From the discussion above, it was evident that the thermal shrinkage of NBMs decreased with the increasing content of nano-SiO_2 particles.

Permeability of NBMs

Porosity and through-hole rate of NBMs are considered as the main index factor of PWF.[24] Figure 9 shows the relationship between PWF and the amount of nano-SiO_2 particles. As shown in Figure 9, PWF increased at first and then decreased with the increasing content of nano-SiO_2 particles. When the amount of nano-SiO_2 particles was 1%, PWF reached a maximum value of 142 Lm^{-2} h^{-1}.

CONCLUSIONS

NBMs with different content of nano-SiO_2 particles were prepared via TIPS process. The experiment results showed that the microporous structure of NBMs was significantly influenced by the different content of nano-SiO_2 particles due to nano-SiO_2 particles affected the phase separation of the blend solution system and severed as nucleating agent to improve the crystallinity of polymers. The thermal shrinkage performance of NBMs decreased with the increasing content of nano-SiO_2 particles because nano-SiO_2 particles was packaged by UHMWPE and HDPE intertwined molecular chains which could reinforce the structural strength of microporous skeleton and hinder the movement of molecular chains. However, the porosity, PWF, and crystalline of NBMs increased at first and then decreased with the increasing content of nano-SiO_2 particles. When the content of nano-SiO_2 particles was 1%, the comprehensive properties of NBMs were optimum.

REFERENCES

1. Arora, P.; Zhang, Z. *Chem. Rev.* **2004**, *104*, 4419.
2. Zhang, S. S. *J. Power Sources* **2007**, *164*, 351.
3. Ryou, M. H.; Lee, Y. M.; Park, J. K.; Choi, J. W. *Adv. Mater.* **2011**, *23*, 3066.
4. Park, J. H.; Cho, J. H.; Park, W.; Ryoo, D.; Yoon, S. J.; Hun Kim, J.; Uk Jeong, Y.; Lee, S.Y. *J. Power Sources* **2010**, *195*, 8306.
5. Kim, K. J.; Kim, J. H.; Park, M. S.; Kwon, H. K.; Kim, H.; Kim, Y. J. *J. Power Sources* **2012**, *198*, 298.
6. Ko, M.; Min, B. G.; Kim, D. W.; Ryu, K. S.; Kim, K. M.; Lee, Y. G.; Chang, S. H. *Electrochim. Acta* **2004**, *50*, 367.
7. Gao, K.; Hu, X. G.; Yi, T. F.; Dai, C. S. *Electrochim. Acta* **2006**, *52*, 443.
8. Roh, S. C.; Park, M. J.; Yoo, S. H.; Kim, C. K. *J. Membr. Sci.* **2012**, *411*, 201.

9. Guan, L.; Jiménez, M. E. G.; Walowski, C.; Boushehri, A.; Prausnitz, J. M.; Radke, C. J. *J. Appl. Polym. Sci.* **2011**, *122*, 1457.
10. Liu, S. J.; Zhou, C. X.; Yu, W. *J. Membr. Sci.* **2011**, *379*, 268.
11. Matsuyama, H.; Yuasa, M.; Kitamura, Y.; Teramoto, M.; Lloyd, D. R. *J. Membr. Sci.* **2000**, *179*, 91.
12. Matsuyama, H.; Maki, T.; Teramoto, M.; Asano, K. *J. Membr. Sci.* **2002**, *204*, 323.
13. Shi, F. M.; Ma, Y. X.; Ma, J.; Wang, P. P.; Sun, W. X. *J. Membr. Sci.* **2012**, *389*, 522.
14. Shi, F. M.; Ma, Y. X.; Ma, J.; Wang, P. P.; Sun, W. X. *J. Membr. Sci.* **2013**, *427*, 259.
15. Li, D. M.; Krantz, W. B.; Greenberg, A. R.; Sani, R. L. *J. Membr. Sci.* **2006**, *279*, 50.
16. Vaisman, L.; Gonza´lez, M. F.; Marom, G. *Polymer* **2003**, *44*, 1229.
17. Cui, A. H.; Liu, Z.; Xiao, C. F.; Zhang, Y. F. *J. Membr. Sci.* **2010**, *360*, 259.
18. Jeong, H. S.; Kim, D. W.; Jeong, Y. U.; Lee, S. Y. *J. Power Sources* **2010**, *195*, 6116.
19. Li, N. N.; Xiao, C. F.; Mei, S.; Zhang, S. *J. Desalinat.* **2011**, *274*, 284.
20. Ma, Y. X.; Shi, F. M.; Ma, J.; Wu, M.; Zhang, J.; Gao, C. *Desalination* **2011**, *272*, 51.
21. Chrissafis, K.; Paraskevopoulos, K. M.; Pavlidou, E.; Bikiaris, D. *Thermochim. Acta* **2009**, *485*, 65.
22. Matsuyama, H.; Teramoto, M.; Kudari, S.; Kitamura, Y. *J. Appl. Polym. Sci.* **2001**, *82*, 169.
23. Witte, P. V. D.; Dijkstra, P. J.; Berg, J. V. D.; Feijen, J. *J. Polym. Sci. B: Polym. Phys.* **1997**, *35*, 763.
24. Han, M. J.; Nam, S. T. *J. Membr. Sci.* **2002**, *202*, 55.